EQUALIZATION OF NONLINEAR SYSTEMS MODELED USING THE BURGERS EQUATION

Shreyas Srikanth Payal[⋆]*, V. John Mathews*

Dept. of Electrical and Computer Engineering, University of Utah, Salt Lake City, UT 84112, USA

ABSTRACT

This paper describes a model-based corrector for distortions due to propagation of acoustic waveforms in air in a cylindrical waveguide at high sound pressure levels. The nonlinear distortions are modeled using the Burgers' wave propagation model, accounting for dissipation and boundary layer dispersion effects. The corrector was designed to mitigate these distortions in signals obtained from predefined distances in the waveguide. This compensator is derived from the Burgers' model and is independent of the stimulus used. Results demonstrating a substantial reduction in the intermodulation distortion and harmonic distortion in a specific frequency band of interest over a multitude of test input stimuli are included in this paper.

Index Terms— nonlinear acoustics, nonlinear distortion, inverse problems, backpropagation algorithms, nonlinear systems.

1. INTRODUCTION

High sound pressure levels (SPL) waveforms suffer 'wave steepening' distortion [1] as these propagate through air. These waveforms are attenuated by the thermoviscous properties of air. As these acoustic waveforms propagate through a waveguide, additional dissipation and dispersion is introduced via interactions of these waves with the walls of the waveguide [2] (Ch. 3, 5), [3]. The objective of this paper is to correct for distortions introduced by the wave propagation at specific observation points.

Waves propagate in air via compressions and rarefactions of air molecules. Due to the properties of the medium and the adiabatic gas laws for air [2] (Ch 2.), [1], the actual speed of sound is a function of these sound pressure levels, the ratio of specific heats for air and the air density.

Figure 1 shows measurements that demonstrate the effects of wave propagation. Distortions introduced during propagation of sinusoidal waveforms of different frequency components over a propagation distance of 3 m are shown in Figure 1. We assume that the driver is coupled with a cylindrical waveguide, allowing for the use of the planar wave propagation assumption in our tests. The dashed red curves correspond to 4 kHz., 6.3 kHz. and 8 kHz. signals measured at a distance of 3 m from the source. The measurements were obtained by applying sinusoidal stimuli through the system such that they are at 135 dB SPL at 3 m. The near-driver measurement (made at a distance of 25.4mm) is presented as the bold blue curve as reference.

Pressure waveforms experience three fundamental physical phenomena during propagation. First, a nonlinear mechanism that introduces harmonic and intermodulation distortion modifying the shape of the waveform. From the principal of conservation of energy, these distortions are generated at the cost of a reduction in the energy contained in the fundamental tone in the stimulus [1]. Attenuation and dispersion are introduced in the waveforms via the thermoviscous properties of air and the waveguide coupled to the acoustic source.

The generation of intermodulation and harmonic distortion stems from the variation in the speed of sound with SPL of the propagating waveform [1]. This paper presents a method to mitigate the effects of this distortion by creating a corrector, which uses the Burgers' propagation model for planar waves to model the distortions. This method be used as a post/pre-compensator. The corrector propagates the waveform in the opposite direction, i.e., the wave propagates from the observation point to the acoustic source. This results in the steepening of these waveforms in a direction opposite to what was observed in traditional wave propagation. Our results indicate a reduction in the harmonic distortion and intermodulation distortion over a wide band of frequencies.

The rest of this paper is organized as follows: Section 2 reviews prior literature in this area. Section 3 first describes the Burgers model for planar acoustic wave propagation. This model leads to a backpropagation-based corrector. An overview of the experimental setup, implementation details and results using this corrector is contained in Section 4. Conclusions and future work are provided in Section 5.

2. LITERATURE REVIEW

Klippel used the Webster horn equation to model nonlinear wave propagation [4] and then constructed a truncated Volterra series based compensator for propagation distortion in [4,5]. This compensator was implemented as a lattice structure. Czerwinksi et. al. presented an implicit implementation of the Poisson solution to compensate for propagation of sinusoidal waveforms emanating out of horn drivers in [6]. They

⋆ email: shreyas.payal@utah.edu.

978-0-9928626-3-3/15/$31.00 ©2015 IEEE

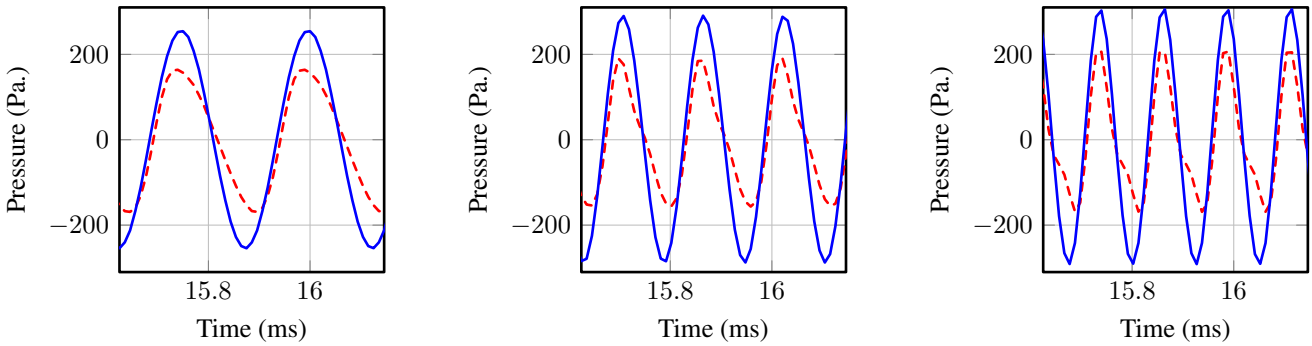

(a) 4 kHz. (b) 6.3 kHz. (c) 8 kHz.

Fig. 1. Comparison of the signals at the source (bold-blue) to those at 3 m (dashed-red) for sinusoidal waveforms with frequency (a) 4 kHz., (b) 6.3 kHz. and (c) 8 kHz. The 3 m signals are at $\approx$ 135 dB SPL (relative to 20 μ Pa.).

also demonstrated the use of the Khokhlov-Zabolotskaya-Kuznetsov (KZK) equation to model wave propagation in a rectangular waveguide. In a recursive manner, over five iterations of measuring predistorted sinusoidal input signals, they were able to reduce the total harmonic distortion introduced by the wave propagation in this rectangular waveguide. Digital backpropagation was first applied in [7] to compensate for distortion introduced by ultrasonic wave propagation in abdominal tissues. The corrector backpropagates a frequency domain representation of the wave-field. Reference [8] describes an iterative method applied to distortion compensation for horn waveguides by propagating the waveform backwards from the mouth to the throat of the horn.

We use a Burgers' model-based compensator, accounting for the effects of waveguide wall on the signal. These boundary-layer effects were not included in the iterative implementation presented in [6]. As pointed out in [6], the combination of signals from different iterations will result in new distortion products that corrupt the audio signal fidelity. Our focus in this paper will be on the pre-compensation of nonlinear distortion to enhance the acoustic signals obtained at pre-defined distances from the source.

3. PROPAGATION MODEL

The Burgers' equation is a partial differential equation (PDE) used to describe wave propagation assuming progressive planar waves [2] (Ch. 5), [9]. The Burgers' model may be formulated as a boundary-value problem (a signal $p(x=0,t)$ is defined for $x=0$, it is desired to compute the pressure, $p(x_l,t)$, at a specific distance x_l, $x_l>0$) using Lagrangian coordinates as [2] (Ch. 3)

$$\frac{\partial p(x,\tau)}{\partial x} = \frac{\beta p(x,\tau)}{\rho_0 c_0^3}\frac{\partial p(x,\tau)}{\partial \tau} + \frac{\delta}{2c_0^3}\frac{\partial^2 p(x,\tau)}{\partial \tau^2} - b\sqrt{\frac{2}{\pi}}\left(\frac{\partial p(x,\tau)}{\partial \tau} * \frac{1}{\sqrt{\tau}}\right) \quad (1)$$

where p corresponds to the pressure field at a location x. The speed of sound for unperturbed air is given by c_0. The Burgers' equation uses τ corresponding to the moving time frame of reference ($\tau = t - \frac{x}{c_0}$). The parameter β is the coefficient of nonlinearity computed as $\beta = \frac{1}{2}(\gamma+1)$, where γ is the ratio of specific heats for an adiabatic process. The parameter ρ_0 denotes the air density of undisturbed air and δ corresponds to the sound diffusivity of air. The boundary layer parameter b is a function of the dimensions of the waveguide and of medium (in this case, air). This last term on the right hand side of (1) arises from the assumption of a thin boundary layer in comparison to the diameter of the waveguide. Reference [10] uses fractional derivatives to compute this term. This is replaced here with the convolution operation ($*$). The parameters δ and b are computed as

$$\delta = \nu\left(\frac{4}{3} + \frac{\mu_B}{\mu} + \frac{\gamma-1}{Pr}\right), \quad (2)$$

$$b = \frac{1}{2R}\sqrt{\frac{2\nu}{c_0^2}}\left[1 + \frac{\gamma-1}{\sqrt{Pr}}\right] \quad (3)$$

Here, ν is the kinematic viscosity, Pr is the Prandtl constant, μ and μ_B correspond to the shear and bulk viscosities, respectively and R is the radius of the cylindrical waveguide. This wave steepening effect is obtained by the first term on the right hand side of (1). The second and third terms in (1) contribute to the effects of the dissipation and dispersion. Equation (1) needs to be solved numerically as there exists no analytical solution [2] (Ch. 5).

3.1. Digital backpropagation based corrector for nonlinear wave propagation

Let us define a digital-backpropagation-based corrector that propagates the waveform in a backward direction for some pre-specified distance. This is expressed as a modified Burgers' model as,

$$\frac{\partial p(x,\tau)}{\partial x} = -1 \times \left[\frac{\beta p(x,\tau)}{\rho_0 c_0^3}\frac{\partial p(x,\tau)}{\partial \tau} + \frac{\delta}{2c_0^3}\frac{\partial^2 p(x,\tau)}{\partial \tau^2} - b\sqrt{\frac{2}{\pi}}\left(\frac{\partial p(x,\tau)}{\partial \tau} * \frac{1}{\sqrt{\tau}}\right)\right] \quad (4)$$

Observe that the right hand side is the same as the Burgers' model in (1) except for the multiplier, -1. This con-

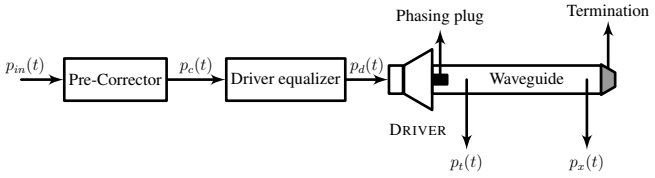

Fig. 2. Hardware for experiments.

struction is equivalent to the design of a nonlinear inverse of the propagation model. This simple structure of the corrector thus retains the distortion generation mechanism. It also includes terms that contribute to the inverse of the attenuation and the compensation of the dispersion generation processes. The corrector attempts to force the wave to steepen in the opposite direction as compared to traditional wave propagation. If the post-corrector was applied to the measured outputs recorded at some distance x_p from the acoustic source, the signal recorded at some other point at a distance x_o from the observation point in the waveguide will be identical to the signal obtained at the output of the post-corrector assuming the same distance (x_o) of virtual propagation from the observation point. This approach can be used to pre- or post-compensate for distortions assuming a pre-specified propagation distance. We do not provide proofs here because of page limitations.

4. PERFORMANCE EVALUATION

4.1. Implementation details

We constructed the compensator as an explicit implementation using a grid in space and time. We used finite differences (FD) to construct the required derivatives of the pressure signal with respect to the distance x and the retarded time τ. The Courant-Friedrichs-Lewy (CFL) condition was maintained when choosing the grid spacing to ensure stability of the numerical implementation [11]. The grid spacing was chosen so as to allow the variation of the speed of sound to some upper bound, c_{max}. The grid spacing was computed as $\Delta x \geq c_{max}\Delta t$ [11], where Δt was chosen to be the sampling time. The Runge-Kutta algorithm was used for spatial integration [12]. The parameter values of the model were chosen as given in [13] and are summarized in Table 1. The convolution operation was implemented as multiplications in the frequency domain.

Table 1. Parameters values for the equalizer.

R	12.7mm	β	1.2 (dimensionless)
c_0	346.57 m s^{-1}	γ	1.4 (dimensionless)
c_{max}	$2c_0$	Pr	0.707 (dimensionless)
Δx	7.2 mm	δ	3.84×10^{-5} m^{2}s^{-1}
P_0	101325 Pa	ν	1.53×10^{-5} m^{2}s^{-1}
ρ	1.2 kg m^{-3}	b	0.000929862 m^{-1}s
μ_B	0.6μ	μ	18.46×10^{-6} kg m^{-1} s^{-1}

4.2. Experimental setup

Figure 2 describes the schematic of the setup used for our evaluations. The driver was coupled to a cylindrical waveguide of diameter $2R = 25.4$mm. The waveguide was assumed to be terminated such that no reflections are fed back into the waveguide. The driver output is denoted by $p_t(t)$. We recorded signals $p_x(t)$ at specific distances from the driver. If the pre-compensator was applied to predistort the input signal, the resulting measurement, called $p_{x_c}(t)$, should ideally be identical to the signal $p_{in}(t)$. We included a band-limited equalizer to compensate for the linear response of the driver [14]. We assumed a perfect driver that does not introduce any nonlinear distortions at these SPL levels. In the absence of the pre-corrector, the input stimulus was applied to the driver equalizer. All measurements from the waveguide were bandlimited (by the sound card used for data acquisition) in these experiments to a range 800 Hz. - 20 kHz. The corrector input was also band-limited to this frequency range.

4.3. Evaluation

We compare the waveforms with and without correction at a distance of 3 m. The testing stimuli contained sinusoids at 4 kHz., 6.3 kHz. and 8 kHz. signals and two multitone signals sampled at 96 kHz.

Figure 3 describes the results of applying this corrector to the three sinusoidal input waveforms. The time domain waveforms corresponding to the pre-corrected measurement signals were very similar to that of the ideal source signals for the 4 kHz. and 6.3 kHz. cases. For the 8 kHz. tones, we see clear discrepancies between the corrected and the ideal. Table 2 shows the normalized root-mean-square error (NRMSE) comparing the ideal to the pre-corrected and the 3 m measurement waveforms. This indicated that the Burgers' model may be inadequate to fully characterize the propagation distortion in cylindrical waveguides at high frequencies.

Figure 4 shows the estimated spectra of the measurements for sinusoidal stimuli. The plots are constructed such that the overlays are shifted along the frequency axis by 50 Hz. This enables easier visualization of the different spectral levels contained in the three signals in each plot. We see that the corrector reduced the second and third-order harmonic distortion by $\approx$ 7 and 20 dB SPL, respectively for the 4 kHz. case and $\approx$ 4 and 14 dB SPL, respectively for the 6.3 kHz. case. As can be expected from Figure 4c, we see minimal reduction for the 8 kHz. case (second harmonic was reduced by $\approx$ 1 dB SPL). Figures 5a-b, compares the total harmonic distortion (THD) (relative to the fundamental frequency) computed for the first 30 harmonics in the bands of interest for the 3 m measurement and the pre-corrected signal. The THD was computed as the ratio of the root-mean-square value of the spectral powers of the harmonics in the frequency range of interest to the power contained in the fundamental frequency component in the distortion-free signal. For the 4 kHz. signal, the corrector reduced the THD from 7.29% to 0.95% for the 133 dB SPL case and from 9.16% to 1.48% for the 135 dB SPL case. This reduction in THD was lower at higher frequencies. For the 8 kHz. measurements, the compensation reduced the THD from 29.7% to 26.3% for the 133 dB SPL

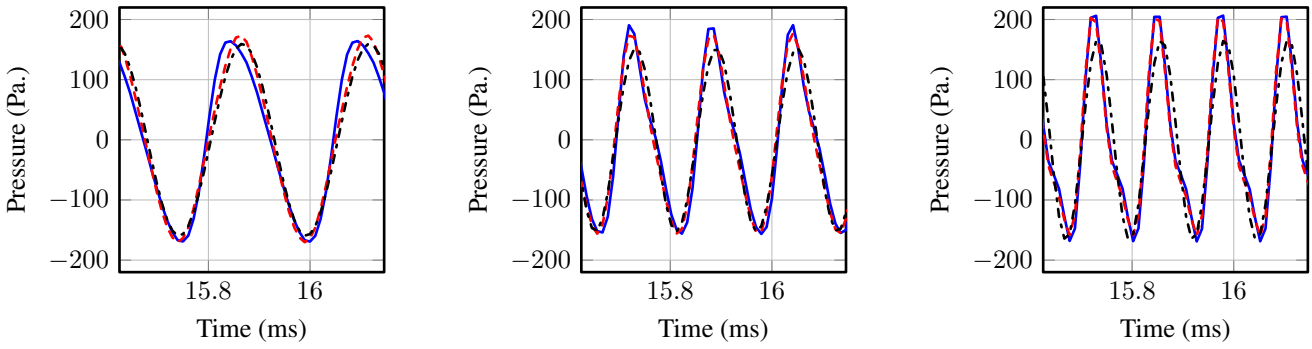

(a) 4 kHz. (b) 6.3 kHz. (c) 8 kHz.

Fig. 3. Comparison of the ideal (dashed-dot-black), the corrected (dashed-red) and 3 m uncorrected output (blue) signals for different frequencies. The measurements were made at ≈ 135 dB SPL (relative to 20 μ Pa.).

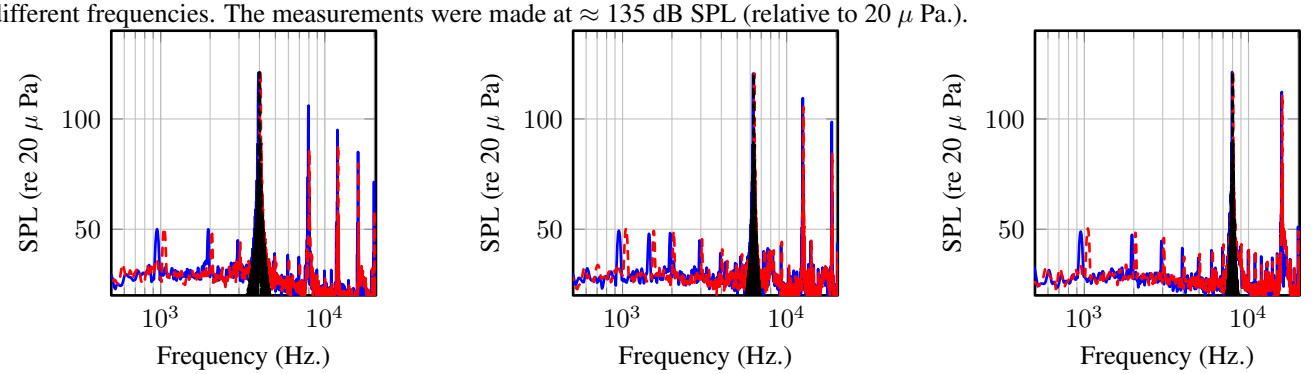

(a) 4 kHz. (b) 6.3 kHz. (c) 8 kHz.

Fig. 4. Comparison of the spectra of the ideal (dash-dot-black), 3 m uncorrected output (bold-blue) and the corrected (dashed-red) signals for different frequencies. These measurements were made at ≈ 135 dB SPL (relative to 20 μ Pa.) at 3 m.

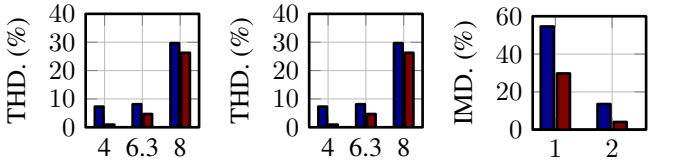

(a) 133 dB SPL (b) 135 dB SPL (c) 134 dB SPL

Fig. 5. Performance metrics for the 3 m uncorrected (blue) and Precorrected (brown) signals : THD for the sinusoidal signals 3 m output. Reduction in the IMD as a percentage of the distortion-free signal power. The measurements were made at the specified SPL levels (relative to 20 μ Pa.) at 3 m.

case and from 34.2% to 30.6% for the 135 dB SPL case as reported in Figures 5a-b.

Figure 6 describes the performance of the corrector for two different multitone stimuli. The corresponding reduction in the intermodulation distortion (IMD) is displayed in Figure 5c. The intermodulation distortion was computed as a ratio of the root-mean-square value of the spectral power contained in the intermodulation products in the frequency band of interest to the root-mean-square value of the power contained in the stimulus frequencies. The nature of the generation of the intermodulation products is determined by the tones present

Table 2. NRMSE(I-ideal, P-precorrected, 3 m-uncorrected)

dB SPL	133	133	135	135
Freq (kHz.)	3 m vs I (%)	P vs I (%)	3 m vs I (%)	P vs I (%)
4	14.69	2.09	18.48	3.08
6.3	23.08	13.30	28.37	17.00
8	29.87	26.62	34.49	31.06

in the input stimulus [15].

From Figure 6a, we observed a reduction in intermodulation distortion of the order ≈5-15dB SPL (the corrector reduced the IMD from 54.6% to 29.8%) . From Figure 6b, this intermodulation distortion reduction is ≈10-20 dB SPL (the corrector reduced the IMD from 13.6% to 4.08%). We were able to perceive this reduction in intermodulation distortion for both signals in our listening tests.

Possible sources of errors in the model include the violation of the planar wave propagation assumption. This assumption is not valid above the resonant frequency of the tube ($f_R = \frac{c_0 \alpha_1}{2\pi R} = 16.6$kHz.) or if, near the driver, the velocity components of the signal in the transverse direction be comparable to those in the direction of wave propagation [16]. Secondly, the driver was not perfectly linear at these SPL levels in our experiments. Thirdly, the cascade of the driver and

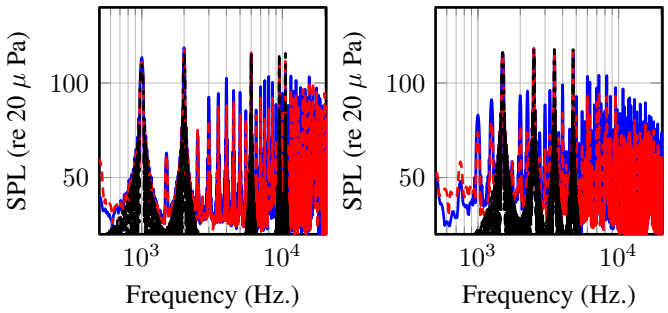

(a) Multitone 1 (b) Multitone 2

Fig. 6. Comparison of the spectra for measured output signals for multitone input signals : ideal (dash-dot-black), 3 m output (bold-blue) and corrected (dashed-red) signals. These measurements were made at $\approx$ 134 dB SPL (relative to 20 μ Pa.) at 3 m.

its equalizer form a band-pass filter that eliminated some distortion products outside this band of interest. This reduced the overall effectiveness of the corrector in that some of these attenuated distortion products were required to compensate for propagation distortion. We also used a non-ideal sound card for data acquisition. Finally, complexity-accuracy trade offs in the FD implementations may govern the quality of the corrected signals. Even with these limitations, this form of compensation guarantees a reduction of intermodulation and harmonic distortion with distance of propagation.

5. CONCLUSIONS AND FUTURE WORK

This paper described a backpropagation-based compensation algorithm for nonlinear propagation distortion in a cylindrical waveguide. Experimental evaluations demonstrated a substantial reduction in harmonic and intermodulation distortions particularly at lower frequencies. This approach could be used as a pre-processing block to reduce the overall distortion introduced by wave propagation with distance. We are currently extending these ideas to non-cylindrical configurations of acoustic waveguides and to cases where the planar wave propagation assumption is not valid.

6. ACKNOWLEDGMENTS

The authors thank the anonymous reviewers for their comments and feedback.

7. REFERENCES

[1] W. Lauterborn, T. Kurz, and I. Akhatov, "Nonlinear acoustics in fluids," in *Springer Handbook of Acoustics*, T.D. Rossing, Ed., pp. 257–297. Springer New York, 2007.

[2] M. F. Hamilton and D. T. Blackstock, *Nonlinear acoustics*, Academic Press, San Diego, CA, USA, first edition, 1998.

[3] F. M. Pestorius, *Propagation of Plane Acoustic Noise of Finite Amplitude*, Ph.D. dissertation, University of Texas at Austin, Austin, TX, 1973.

[4] W. Klippel, "Nonlinear wave propagation in horns and ducts," *J. Acoust. Soc. Am.*, vol. 98, no. 1, pp. 431–436, Mar 1995.

[5] W. Klippel, "Compensation for nonlinear distortion of horn loudspeakers by digital signal processing," *J. Audio Eng. Soc*, vol. 44, no. 11, pp. 964–972, Nov 1996.

[6] E. Czerwinski, A. Voishvillo, S. Alexandrov, and A. Terekhov, "Propagation distortion in sound systems: Can we avoid it?," *J. Audio Eng. Soc*, vol. 48, no. 1/2, pp. 30–48, Feb 2000.

[7] D. Liu and R. C. Waag, "Correction of ultrasonic wavefront distortion using backpropagation and a reference waveform method for time shift compensation," *J. Acoust. Soc. Am.*, vol. 96, no. 2, pp. 649–660, Apr 1994.

[8] K. R. Holland and C. L. Morfey, "A model of nonlinear wave propagation in horns," *J. Audio Eng. Soc*, vol. 44, no. 7/8, pp. 569–580, July 1996.

[9] B. Enflo and C. M Hedgerg, *Theory of nonlinear acoustics in fluids*, Springer, London, UK, first edition, 2002.

[10] D. T. Blackstock, "Generalized Burgers equation for plane waves," *J. Acoust. Soc. Am.*, vol. 77, no. 6, pp. 2050–2053, Mar 1985.

[11] R. Courant, K. Friedrichs, and H. Lewy, "On the partial difference equations of mathematical physics," *IBM J. Res. Dev.*, vol. 11, no. 2, pp. 215–234, Mar. 1967.

[12] J. D. Lambert, *Numerical Methods for Ordinary Differential Systems: The Initial Value Problem*, John Wiley & Sons, Inc., New York, NY, USA, first edition, 1991.

[13] A. Pierce, *Acoustics : an introduction to its physical principles and applications*, Mc Graw-Hill, Inc, New York, NY, USA, first edition, 1981.

[14] A. Carini, V. J. Mathews, and G. L. Sicuranza, "Equalization of recursive polynomial systems," *IEEE Signal Processing Letters*, vol. 6, no. 12, pp. 312–314, December 1999.

[15] A. Voishvillo, A. Terekhov, E. Czerwinski, and S. Alexandrov, "Graphing, interpretation, and comparison of results of loudspeaker nonlinear distortion measurements," *J. Audio Eng. Soc*, vol. 52, no. 4, pp. 332–357, Apr 2004.

[16] P. Konicek, M. Bednarik, and M. Cervenka, "Propagation of quasi-plane nonlinear waves in tubes," *Acta Polytechnica*, vol. 42, no. 4, 2002.